CHINESE MEDICINE

RESEARCH

Open Access

CrossMark

Crude triterpenoid saponins from *Ilex latifolia* (*Da Ye Dong Qing*) ameliorate lipid accumulation by inhibiting SREBP expression via activation of AMPK in a non-alcoholic fatty liver disease model

Rui-Bing Feng[1,2†], Chun-Lin Fan[1,2†], Qing Liu[1,2†], Zhong Liu[3], Wei Zhang[1,2], Yao-Lan Li[1,2], Wei Tang[1,2], Ying Wang[1,2*], Man-Mei Li[1,2*] and Wen-Cai Ye[1,2*]

Abstract

Background: *Ilex latifolia* Thunb. (*Da Ye Dong Qing*) is used for weight loss and for its antidiabetic effects. This study aims to investigate the beneficial effects and potential mechanisms of action of crude triterpenoid saponins (CTS) from *I. latifolia* in a mouse model of high-fat diet (HFD)-induced non-alcoholic fatty liver disease (NAFLD).

Methods: Male C57BL/6 mice (n = 50), were arbitrarily divided into five groups (n = 10 in each group): a control group, HFD group, simvastatin group (10 mg/kg/day), and two CTS treatment groups (100 and 200 mg/kg/day). All mice except those in the control group were fed an HFD for 4 weeks. Animals in the treatment groups were orally administered simvastatin or CTS for 8 weeks. Oral glucose tolerance tests and insulin tolerance tests were performed. At the end of treatment, plasma lipid levels, and oxidative parameters in the liver were measured using commercial test kits. Western blotting was used to evaluate whether CTS induced AMP-activated protein kinase (AMPK) and acetyl CoA carboxylase activation, and the expression of transcription factors and their target genes was evaluated in a quantitative PCR assay.

Results: Compared with the HFD group, the CTS (200 mg/kg/day) treatment group showed significantly decreased plasma lipid parameters (P < 0.001, P = 0.018, and P = 0.005 for triglycerides, total cholesterol and low-density lipoprotein cholesterol, respectively), and improved insulin resistance (P = 0.006). CTS (100 and 200 mg/kg/day) supplementation also reduced hepatic lipids and protected the liver from oxidative stress by attenuating malondi-aldehyde content (P < 0.001 and P < 0.001, respectively) and restoring aspartate aminotransferase levels (P < 0.001 and P < 0.001, respectively). Moreover, CTS (200 mg/kg/day) reduced lipid accumulation by enhancing AMPK phosphorylation and inhibiting expression of sterol regulatory element-binding proteins (SREBPs) and their target genes SREBP-1c, SREBP-2, fatty acid synthase, and stearoyl-CoA desaturase (P = 0.013, P = 0.007, P = 0.011, and P = 0.014, respectively).

Conclusion: CTS from *I. latifolia* improved insulin resistance and liver injury in HFD-fed mice, and attenuated NAFLD via the activation of AMPK and inhibition of the gene expression of SREBPs and some of their target molecules.

*Correspondence: wangying_cpu@163.com; limanmei@hotmail.com; chyewc@gmail.com
†Rui-Bing Feng, Chun-Lin Fan and Qing Liu contributed equally to this study
[1] College of Pharmacy, Jinan University, Guangzhou 510632, People's Republic of China
Full list of author information is available at the end of the article

BioMed Central

Feng *et al. Chin Med* (2015) 10:23

Page 2 of 13

Background

Non-alcoholic fatty liver disease (NAFLD) is characterized by fatty changes in the liver that do not occur as a result of alcohol intake. It refers to a wide spectrum of conditions involving liver damage, including non-alcoholic steatohepatitis (NASH), fibrosis, and cirrhosis and its complications [1, 2], and is now regarded as a manifestation of metabolic syndrome and a shared pathogenic factor for obesity, type 2 diabetes mellitus (T2DM), and cardiovascular disease [3, 4]. In terms of its pathogenesis, excessive fat accumulation in hepatic cells causes oxidative stress in the liver, leading to the development of insulin resistance (IR) [5, 6]. Thus, reducing fat accumulation by inhibiting lipogenic synthesis and increasing fat breakdown could be helpful in the prevention and treatment of NAFLD.

Many enzymes and transcription factors are involved in lipogenesis and are organized into multi-enzyme complexes to promote fatty acid synthesis, including acetyl CoA carboxylase (ACC), fatty acid synthase (FAS), stearoyl-CoA desaturase 1 (SCD-1), and sterol regulatory element-binding protein (SREBP) [7, 8]. In the liver, SREBP-2 predominantly regulates enzymes associated with cholesterol and bile acid synthesis, such as hydroxymethylglutaryl coenzyme A synthase (HMGCS) [9]. AMP-activated protein kinase (AMPK) is a serine/threonine protein kinase composed of α, β, and γ subunits, and is associated with adipocyte differentiation [10]. Furthermore, increasing evidence indicates an inverse correlation between AMPK and SREBP-1c in hepatocytes and the livers of high-fat diet (HFD)-fed or ethanol-fed mice [11, 12]. AMPK interacted with and phosphorylated SREBP-1c and SREBP-2 to attenuate hepatic steatosis in mice with diet-induced IR [13]. Therefore, the regulation of AMPK and SREBP may be of key therapeutic importance in preventing fatty liver disease.

The leaves of *Ilex latifolia* Thunb. (*Da Ye Dong Qing*) have been widely used to quench thirst, refresh the mind, relieve *wind-heat* (*feng-re*), and clear toxins from the *blood* (*xue*); they are also used to treat the common cold, obesity, sore throat, rhinitis, itching eyes, and conjunctival congestion [14]. Furthermore, *I. latifolia* may improve hypertension, hyperlipidemia, and other cardiovascular diseases [15, 16]. Phytochemical studies have indicated that triterpenoids, phenolic acids, flavonoids, and essential oils are the major constituents of *I. latifolia* [17–19]. Many of these components have potential health benefits including antioxidant, anti-obesity, neuro-protective, hepatoprotective, and anti-inflammatory effects [20–23]. Triterpenoids from *I. latifolia* were shown to inhibit acyl CoA cholesterol acyl transference [24].

This study aims to investigate the beneficial effects and potential mechanisms of action of crude triterpenoid saponins (CTS) from *I. latifolia* in a mouse model of HFD-induced NAFLD.

Methods

Plant material

The leaves of *I. latifolia* were collected from Wanning, Hainan Province, China, and were identified by Prof. Guangxiong Zhou, College of Pharmacy, Jinan University, Guangzhou, China. The voucher specimen (No. 1201209) was deposited at the College of Pharmacy, Jinan University.

Chemicals and reagents

Kudinoside O, kudinoside N, kudinoside H, latifoloside G, kudinoside G kudinoside C, kudinoside A, kudinoside E, kudinoside F, latifoloside Q, kudinoside D, and ilekudinoside E were extracted from the leaves of *I. latifolia* using boiling water, separated using D101 macroporous resin (Yunkai Resin Technology Co., Ltd., China) and silica gel column chromatography (Qingdao Haiyang Chemical Co., Ltd., China), and purified using high performance liquid chromatography (HPLC) column chromatography (Cosmosil 5C18-MS-II, Nacalai Tesque, Japan) and a preparative HPLC system (Agilent 1260, Agilent Technologies, USA). The structures of these saponins were determined by comparing their spectral (UV, IR, MS, and NMR) data with those in the literature [15, 25–27]. Each saponin was dissolved in methanol at a concentration of 20 μg/mL. HPLC-grade acetonitrile, methanol, and formic acid were purchased from Merck (Darmstadt, Germany). Rabbit polyclonal antibodies against phospho-AMPKα (Thr172), AMPK, phospho-ACC, and ACC were purchased from Cell Signaling Technology (Danvers, MA, USA). All the other chemical reagents were obtained from Sigma-Aldrich (St. Louis, MO, USA). Normal diets and the HFD were purchased from Guangdong Medical Laboratory Animal Center (Guangzhou, China). The HFD consisted of 18% lard stearin (w/w), 5% egg powder, 1% cholesterol, 20% sucrose, 0.1% bile salt, and 55.9% normal diet.

CTS preparation

The leaves of *I. latifolia* were extracted three times with boiling water for 2 h. The extracting solution was applied to a D 101 resin column and eluted with H_2O, 45% EtOH, 75% EtOH, and 95% EtOH successively to obtain four fractions. Our previous studies, in which we performed a chemical analysis of the leaves of *I. latifolia* using ultra-high-performance liquid chromatography quadrupole time-of-flight mass spectrometry (UPLC-QTOF–MS), showed the presence of CTS in the 75% EtOH fractions [28]. The 75% EtOH fraction was concentrated and dried in a vacuum to obtain the CTS.

Feng *et al. Chin Med* (2015) 10:23

Page 3 of 13

Determination of CTS content

CTS were qualitatively and quantitatively analyzed by UHPLC-Q-TOF-MS. The CTS (20 mg) were dissolved in 100 mL of methanol, and filtered with a 0.22-μm nylon filter membrane. The samples were prepared in triplicate. The filtrate was then transferred to an auto-sampler vial for UHPLC-Q-TOF-MS analysis. The injection volume was 2 μL.

UHPLC was performed on a Waters Acquity UHPLC system (binary solvent delivery system, auto sampler, and column compartment; Waters, Milford, MA, USA), which was coupled with a Waters Xevo G2 Q-TOF (Waters). The samples were separated on an Agilent Extend C18 RRHD column (2.1 × 150 mm I.D., 1.8 μm). The mobile phase consisted of H_2O containing 0.1% formic acid (v/v, solvent A) and acetonitrile containing 0.1% formic acid (v/v, solvent B). A gradient program was used according to the following profile: 0–1 min, 5% B; 1–4 min, 5–25% B; 4–12 min, 25–40% B; 12–13 min, 40–95% B; and 3-min post-run, 5% B, flow rate 0.5 mL/min. The column temperature was 40°C. The interface was electrospray injection, and the acquisition parameters were as follows: capillary voltage, 3,500 V; cone voltage, 5 V; source temperature, 100°C; nebulization gas, 800 L/h at 350°C; cone gas, 50 L/h; and mass range recorded, m/z 100–15,00. During the whole process of analysis, leucine-enkephalin (m/z 554.2615) served as a reference ion was sampled 0.3 s per 5 s. Quantification was performed using the negative ion mode.

Animals and their treatment

Six-week-old, male C57BL/6J mice (n = 50, specific pathogen-free grade, Certified No. SCXK [Guangdong] 2003-0001) were obtained from Guangdong Medical Laboratory Animal Center (China). The animals were kept in a breeding room with controlled environment (temperature: 23 ± 1°C, 12 h dark/light cycle from 6:00 a.m. to 6:00 p.m.) with free access to food and water. After a week of adaptation, the mice were arbitrarily divided into five groups (n = 10/group) as follows: a control group (Control group), an HFD-fed group (HFD group), treatment groups fed the HFD for 4 weeks followed by administration of CTS at 100 mg/kg/day or 200 mg/kg/day, or a positive control group treated with simvastatin (10 mg/kg/day) (Laboratories Fournier S.A., USA) by oral gavage for 8 weeks. During the experiment, animal body weight was recorded each week, and the control and HFD groups received equal volumes of saline for 8 weeks. After 8 weeks of treatment, all animals were sacrificed under chloral hydrate anesthesia and blood was collected by cardiac puncture. The main part of the visceral fat was removed from each group and weighed. The livers and blood plasma were collected and stored at −80°C for further biochemical analysis. All animal experiments were conducted in accordance with the guidelines (publication number 85–23, revised 1996) set by the National Institutes of Health and the U.S. Department of Agriculture, and were approved by the local animal ethics committee of Jinan University.

Oral glucose tolerance test (OGTT)

In a separate trial, glucose tolerance was analyzed as previously described [29]. After 50 days of treatment with the HFD, mice were fasted overnight and orally administered 2 g/kg glucose. Glucose levels were measured in tail blood before and at 30, 60, or 120 min after oral administration using a blood glucose monitoring system (ACCU-CHEK® Active, Roche, Germany). The area under the curve (AUC) of blood glucose and time was calculated according to the following formula:

$$AUC_{0-2\,h} = [(G_{0\,h} + G_{1\,h}) \times 1h + (G_{1\,h} + G_{2\,h}) \times 1h]/2$$

where "G" is the blood glucose value.

Insulin tolerance test (ITT)

The ITT was performed as previously described [29]. After 60 days of treatment with the HFD, mice were fasted overnight and subcutaneously injected with 0.75 U/kg insulin (Novolin, Novo Nordisk, Denmark). Glucose levels were measured from tail blood before and 15, 30, 60, or 120 min after injection with a blood glucose monitoring system (ACCU-CHEK®Active, Roche, Germany). All animals were sacrificed 3 days after the ITT. Plasma insulin levels were measured with the insulin radioimmunoassay kit (North Institute of Biological Technology, China) according to the manufacturer's instructions.

Measurement of biochemical parameters in plasma

Plasma was separated by centrifuge (Eppendorf 5417R; Eppendorf, Germany) at 1,699×g for 15 min at 4°C. The triglyceride (TG) and total cholesterol (TC) contents in plasma were measured using TG and TC quantification kits (Nanjing Jiancheng Bioengineering Institute, China). Blood glucose, low-density lipoprotein cholesterol (LDL-c), and high-density lipoprotein cholesterol (HDL-c) levels were determined according to the protocols of commercially available kits (Nanjing Jiancheng Bioengineering Institute). The enzymatic activities of plasma aspartate aminotransferase (ALT) and alanine aminotransferase (AST) were estimated for assessing liver damage using biochemical kits (Nanjing Jiancheng Bioengineering Institute).

Feng *et al. Chin Med* (2015) 10:23

Page 4 of 13

Assay of hepatic levels of free fatty acid (FFA), glutathione (GSH), malondialdehyde (MDA), and adenosine triphosphatase (ATPase)

The content of FFA in the liver was measured using a commercially available kit according to the manufacturer's protocol (Nanjing Jiancheng Bioengineering Institute). Hepatic tissues were homogenized (10%, w/v) in ice-cold saline (pH 7.4) and centrifuged at $1,699 \times g$ for 10 min at 4°C. The supernatants were transferred to new centrifuge tubes and the MDA, GSH, and ATPase contents were measured using biological test kits. Lipid peroxidation was estimated by measuring thiobarbituric acid-reactive substances (TBARS), and is expressed in terms of MDA content according to the manufacturer's protocol. The reagent products were pink in color and absorbance was measured using an MK3 microplate reader (Thermo Company, MA, USA) at 532 nm. Protein content was determined using a protein assay kit (Bio-Rad Laboratories Inc., USA) to normalize MDA, GSH, and ATPase levels.

Oil red O staining of liver

For microscopic analysis of the effect of CTS treatment on hepatic lipid accumulation induced by the HFD, 0.5 g/100 ml Oil red O (Sigma-Aldrich, St Louis, MO, USA) stock solution was prepared in isopropanol. Liver tissues (5 μm) were frozen, embedded in optimal cutting temperature medium, stained with Oil red O for 15 min and washed, and finally, counterstained with hematoxylin. The samples were photographed and examined using a light microscope (Olympus, Japan) at a magnification of 400×.

Hepatic lipid content analysis

Liver samples from the five groups were weighed and homogenized in tissue lysis buffer containing 20 mM Tris HCl (pH 7.5), 150 mM NaCl, 1% Triton X-100; lipid was extracted with chloroform/methanol (2:1, v/v).The chloroform layers were separated to measure hepatic TG and cholesterol levels using triglyceride and cholesterol kits according to the manufacturer's instructions.

RNA extraction and real-time reverse transcription polymerase chain reaction (RT-PCR)

Total RNA was extracted from mouse liver tissues using Trizol reagent (Invitrogen, Carlsbad, CA, USA) following the manufacturer's directions to determine the effects of CTS on TG- and cholesterol-related gene expression. Reverse transcription (RT) by total RNA (1 μg), oligo (15) dT, and reverse transcriptase was performed using RT kits (Takara Biotechnology, Inc., Shiga, Japan) in a final volume of 50 μL. PCR primer sequences were designed using primer 6.0 software and synthesized by Invitrogen Technologies (China). The gene expression levels were analyzed in duplicate using a SYBR Green kit (Takara Biotechnology, Inc.) on a real-Time PCR System (Light Cycler 480, Roche, Switzerland). All the primer lengths and annealing temperatures are listed in Table 1. The values of the threshold cycle (C_t) were determined using Roche analysis software (Light Cycler 480). The relative gene expression levels were normalized to the GADPH expression level, and the ratios are presented as arbitrary units.

Western blotting analysis

Fresh liver tissues were homogenized and lysed in ice-cold buffer for 30 min, and tissue lysate samples were centrifuged at $15,294 \times g$ for 20 min at 4°C. The supernatants were collected and the protein concentrations of the lysates were measured using a BCA protein assay (Bio-Rad Laboratories Inc.). Twenty micrograms of total protein was separated by 8% SDS–polyacrylamide gel electrophoresis (SDS-PAGE), electrotransferred to a PVDF membrane (Millipore, MA, USA), blocked, and immunoblotted with rabbit polyclonal antibodies specific for phospho-AMPKα, AMPK, phospho-ACC, and ACC (diluted 1:1,000) overnight at 4°C. The blots were incubated with a goat anti-rabbit IgG HRP-conjugated secondary antibody for 2 h at room temperature after being washed. Antibody binding on the PVDF membrane was detected using an enhanced chemiluminescence western blot detection kit (Invitrogen, USA) and Kodak X-ray film.

Statistical analysis

Data were analyzed using Origin version 8.0 software (Origin Lab, USA) and are presented as the

Table 1 Primer sequences used for real-time PCR

Genes		Primer sequences	Length
HMGCS	Forward	(5′-3′) GCCGTGAACTGGGTCGAA	77 bp
	Reverse	(5′-3′) GCATATATAGCAATGTCTCCTGCAA	
ACC	Forward	(5′-3′) TGAAGGGCTACCTCTAATG	182 bp
	Reverse	(5′-3′) TCACAACCCAAGAACCAC	
SCD-1	Forward	(5′-3′) CCGGAGACCCCTTAGATCGA	190 bp
	Reverse	(5′-3′) TAGCCTGTAAAAGATTTCTGCAAACC	
SREBP-2	Forward	(5′-3′)GCGTTCTGGAGACCATGGA	131 bp
	Reverse	(5′-3′) ACAAAGTTGCTCTGAAAACAAATCA	
SREBP-1c	Forward	(5′-3′)TGTTGGCATCCTGCTATCTG	189 bp
	Reverse	(5′-3′) AGGGAAAGCTTTGGGGTCTA	
FAS	Forward	(5′-3′) GCTGCGGAAACTTCAGGAAAT	84 bp
	Reverse	(5′-3′) AGAGACGTGTCACTCCTGGACTT	
GAPDH	Forward	(5′-3′) AGGTCGGTGTGAACGGATTTG	123 bp
	Reverse	(5′-3′) TGTAGACCATGTAGTTGAGGTCA	

Feng *et al. Chin Med* (2015) 10:23

Page 5 of 13

mean ± standard deviation (SD). Student's *t* test was used to compare the difference between two groups, and one-way analysis of variance (ANOVA) was used to perform multiple comparisons. The dose-dependent manner was visually determined from the graphs and the tendency of the data. *P* values less than 0.05 were considered statistically significant and a *P* value less than 0.01 was considered very statistically significant; exact P-values are shown unless *P* < 0.001.

Results

CTS content in *I. latifolia*

There were significant differences in the quantities of the 12 main saponins (Fig. 1; Table 2) The contents of the 12 main saponins were obtained directly using an external standard method. The content of kudinoside D (196.68 mg/g) was the highest, followed by those of kudinoside A (117.97 mg/g), latifoloside H (104.17 mg/g), and kudinoside C (95.57 mg/g). The total amount of the twelve main saponins making up CTS was 861.03 mg/g.

CTS reduce the body, liver, and adipose tissue weights in mice fed the HFD

Compared with the control group, mice fed the HFD for 12 weeks exhibited an obvious increase in body, liver, and adipose tissue (omental adipose tissue, perirenal adipose tissue, epididymal adipose tissue) weights (*P* = 0.007, *P* < 0.001, and *P* < 0.001, respectively). A significantly lower weight gain was observed in the groups treated with CTS-100 mg/kg/day (*P* = 0.037) or CTS-200 mg/kg/day (*P* = 0.022) than in the HFD group. Adipose tissue weight was slightly lower in the CTS-100 mg/kg/day group (*P* = 0.050) than in the HFD group. The liver weight and the ratios of liver to body weight in the HFD group were markedly higher than those in the other groups (*P* < 0.001 and *P* < 0.001, respectively). Compared with the HFD group, the CTS-200 mg/kg/day group showed significantly decreased weight of adipose tissue and ratio of adipose tissue to body weight (*P* = 0.027 and *P* = 0.014, respectively). The HFD induced hepatic steatosis and predominantly increased liver, adipose tissue, and body weights. Treatment with CTS inhibited the progression of hepatic steatosis and weight gain in the liver and adipose tissue (Table 3).

CTS improve plasma lipid parameters in mice fed the HFD

Lipid levels in the blood were measured as shown in Table 4. The plasma TG, TC, and LDL-c levels were markedly higher in the HFD group (1.98 ± 0.54, 6.27 ± 1.38, and 2.80 ± 0.77 μmol/mL, respectively) compared with the control group (1.37 ± 0.46, 2.48 ± 0.23, and 0.32 ± 0.19 μmol/mL) (*P* = 0.050, *P* < 0.001, and

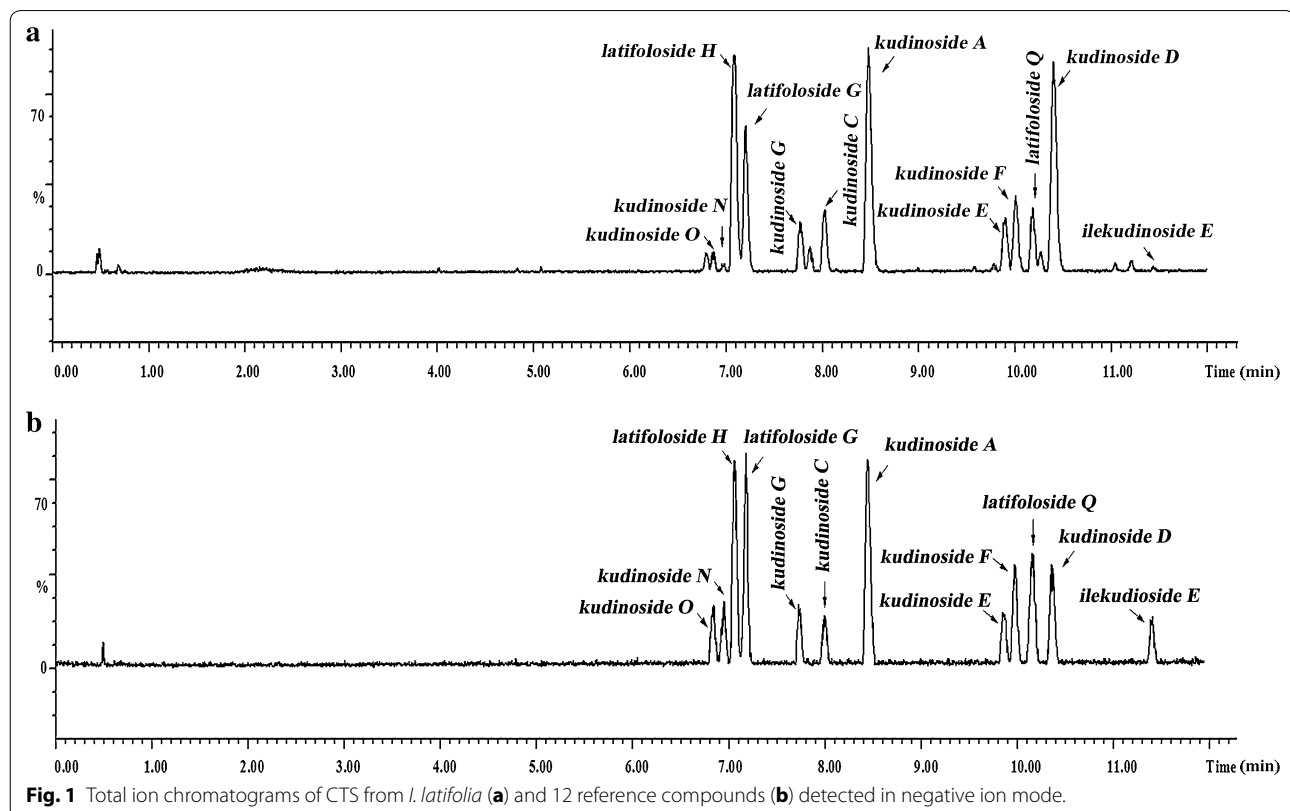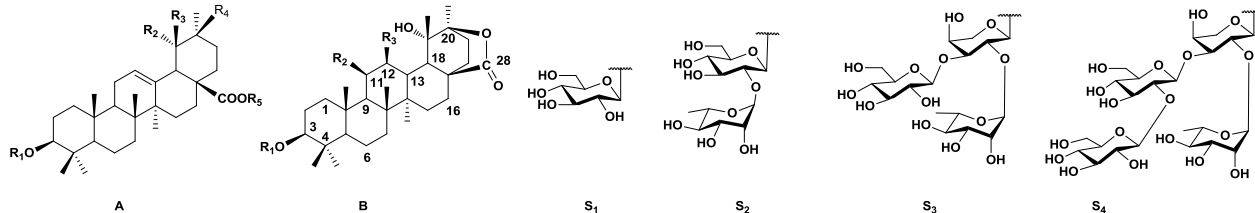**Fig. 1** Total ion chromatograms of CTS from *I. latifolia* (**a**) and 12 reference compounds (**b**) detected in negative ion mode.

Feng *et al. Chin Med* (2015) 10:23

Page 6 of 13

Table 2 The chemical structures and contents of 12 triterpenoid saponins in the extract of *I. latifolia*

No.	Constituents	Structure							Experimental negative QTOF-MS (m/z)/error (ppm)	Weight of concentration (mg/g)
		Type	R$_1$	R$_2$	R$_3$	R$_4$	R$_5$	=		
1	Kudinoside O	A	S$_4$	OH	H	CH$_3$	S$_2$	12 (13)	1381.6641 [M − H]$^-$/0.31	50.63
2	Kudinoside N	A	S$_4$	OH	CH$_3$	H	S$_2$	12 (13)	1381.6632 [M − H]$^-$/0.96	3.45
3	Latifoloside H	A	S$_3$	OH	H	CH$_3$	S$_2$	12 (13)	1265.6165 [M + COOH]$^-$/0.56	104.17
4	Latifoloside G	A	S$_3$	OH	CH$_3$	H	S$_2$	12 (13)	1265.6173 [M + COOH]$^-$/−0.09	45.76
5	Kudinoside G	A	S$_3$	OH	CH$_3$	H	S$_1$	12 (13)	1119.5595 [M + COOH]$^-$/−0.21	65.84
6	Kudinoside C	B	S$_4$	H	OH	–	–	13 (18)	1133.5375 [M + COOH]$^-$/0.96	95.57
7	Kudinoside A	B	S$_3$	H	OH	–	–	13 (18)	971.4853 [M + COOH]$^-$/0.45	117.97
8	Kudinoside E	B	S$_4$	H	H	–	–	11 (12), 13 (18)	1115.5287 [M + COOH]$^-$/−0.68	78.31
9	Kudinoside F	B	S$_3$	OH	H	–	–	13 (18)	971.4848 [M + COOH]$^-$/0.88	61.16
10	Latifoloside Q	A	S$_3$	H	H	CH$_3$	S$_2$	12 (13)	1249.6226 [M + COOH]$^-$/−0.27	33.99
11	Kudinoside D	B	S$_3$	H	H	–	–	11 (12), 13 (18)	953.4759 [M + COOH]$^-$/−0.82	196.68
12	Ilekudinoside G	B	S$_4$	H	H	–	–	12 (13)	1117.5430 [M + COOH]$^-$/0.58	7.50
Crude triterpenoid saponins										861.03

Table 3 Effects of CTS on body weight, liver weight, and adipose tissue weight of mice fed with HFD

Parameter	Control	HFD	HFD + Simvastatin	HFD + CTS-100	HFD + CTS-200
Initial body weight (g)	21.10 ± 1.62	21.22 ± 1.21	20.31 ± 1.03	21.56 ± 2.02	21.64 ± 1.36
Final body weight (g)	30.35 ± 3.06	40.39 ± 3.02$^{\#\#}$	35.63 ± 4.63$^{\triangle}$	37.97 ± 4.13*	37.68 ± 2.91*
Body weight gain (g)	9.25 ± 0.91	19.17 ± 0.32$^{\#}$	15.32 ± 0.53$^{\triangle}$	16.41 ± 0.44*	14.89 ± 0.46*
Adipose tissue^a weight (g)	0.96 ± 0.23	1.67 ± 0.49$^{\#\#}$	1.24 ± 0.29$^{\triangle}$	1.37 ± 0.64	1.43 ± 0.54*
Ratio of adipose tissue and body weight (%)	3.22 ± 0.90	4.29 ± 1.55$^{\#\#}$	3.51 ± 1.49$^{\triangle}$	3.67 ± 2.16	3.84 ± 1.46*
Liver weight (g)	1.45 ± 0.14	2.26 ± 0.17$^{\#\#}$	2.02 ± 0.39$^{\triangle\triangle}$	2.15 ± 0.22	2.09 ± 0.39**
Ratio of liver and body weight (%)	4.81 ± 0.60	5.74 ± 0.71$^{\#\#}$	5.50 ± 1.47$^{\triangle}$	5.70 ± 0.70	5.63 ± 1.30*

Adipose tissue^a : including omental adipose tissue, perirenal adipose tissue, and epididymal adipose tissue.

Values were expressed as the mean ± SD (n = 10). $^{\#}$ $P < 0.05$, $^{\#\#}P < 0.01$, HFD vs. control. $^{\triangle}P < 0.05$, $^{\triangle\triangle}P < 0.01$, HFD vs. simvastatin treatment. *$P < 0.05$, **$P < 0.01$, HFD vs. CTS treatment.

$P < 0.001$, respectively). The plasma concentrations of TG, TC, and LDL-c were lower in the simvastatin-treated group and the CTS-administered groups compared with the HFD group, and the levels of TG, TC, and LDL-c in mice treated with CTS-200 mg/kg/day were significantly lower ($P < 0.001$, $P = 0.018$, and $P = 0.005$, respectively). In contrast, CTS-200 mg/kg/d increased the content of HDL-c, similar to simvastatin, whereas the HFD decreased it ($P = 0.006$). Our results suggested that CTS treatment could reduce fat accumulation in HFD-fed C57BL/6 mice.
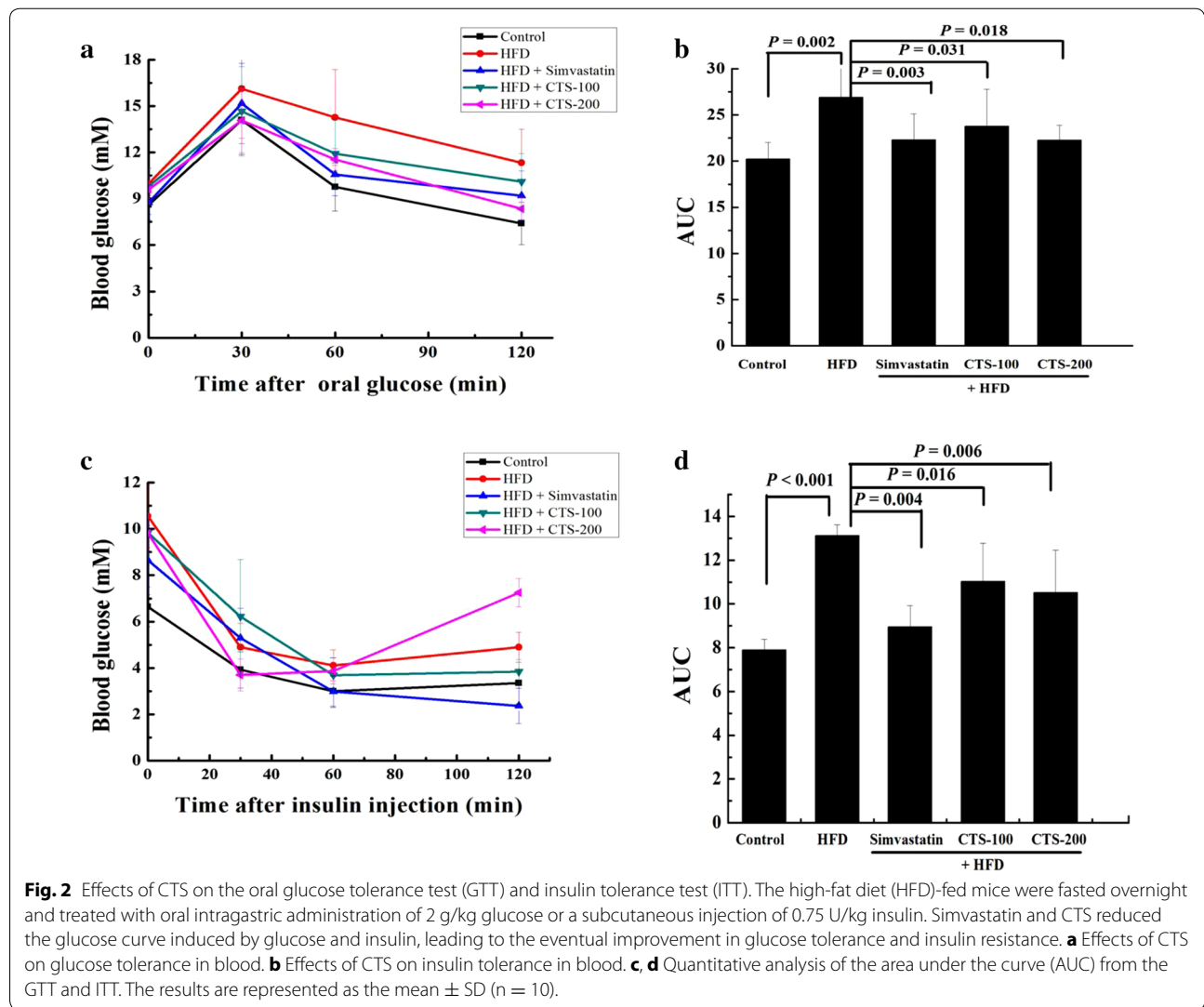
CTS improve IR in mice

After 50 days of CTS treatment, the untreated HFD-fed mice showed a significant increase in blood glucose levels compared with the levels observed in normal controls (Fig. 2a). Simvastatin (10 mg/kg/day) and CTS (100 and 200 mg/kg/day) inhibited this increase in blood glucose levels, and decreased the area under the curve (AUC) of blood glucose over time compared with the AUC for the HFD group ($P = 0.003$, $P = 0.031$, and $P = 0.018$, respectively) (Fig. 2b). Compared with the control group, the HFD-fed mice exhibited impaired insulin

Feng *et al. Chin Med* (2015) 10:23

Page 7 of 13

Table 4 Effects of CTS on plasma parameters in mice fed with HFD

Parameter	Control	HFD	HFD + Simvastatin	HFD + CTS-100	HFD + CTS-200
TG (mmol/L)	1.37 ± 0.46	1.98 ± 0.54[#]	1.04 ± 0.26[△△]	1.29 ± 0.34**	1.21 ± 0.15**
TC (mmol/dL)	2.48 ± 0.23	6.27 ± 1.38[##]	5.27 ± 0.20[△]	5.79 ± 0.60	5.59 ± 0.70*
LDL-C (mmol/dL)	0.32 ± 0.19	2.80 ± 0.77[##]	1.95 ± 0.45[△]	2.53 ± 0.28	2.09 ± 0.39**
HDL-c (mmol/dL)	1.33 ± 0.46	0.95 ± 0.10[#]	1.77 ± 0.66[△]	1.25 ± 0.30**	1.36 ± 0.08**
Glucose (mmol/L)	8.61 ± 1.34	9.99 ± 1.56[##]	8.76 ± 1.43[△]	9.80 ± 1.53	9.60 ± 1.21
Insulin (nmol/L)	22.63 ± 5.93	36.56 ± 7.77[##]	25.53 ± 7.03[△]	26.43 ± 9.71*	24.52 ± 6.20**

Values were expressed as the mean ± SD (n = 10). [#] $P < 0.05$, [##]$P < 0.01$, HFD *vs*. control. [△]$P < 0.05$,[△△]$P < 0.01$, HFD vs. simvastatin treatment. *$P < 0.05$, **$P < 0.01$, HFD vs. CTS treatment.

Fig. 2 Effects of CTS on the oral glucose tolerance test (GTT) and insulin tolerance test (ITT). The high-fat diet (HFD)-fed mice were fasted overnight and treated with oral intragastric administration of 2 g/kg glucose or a subcutaneous injection of 0.75 U/kg insulin. Simvastatin and CTS reduced the glucose curve induced by glucose and insulin, leading to the eventual improvement in glucose tolerance and insulin resistance. **a** Effects of CTS on glucose tolerance in blood. **b** Effects of CTS on insulin tolerance in blood. **c**, **d** Quantitative analysis of the area under the curve (AUC) from the GTT and ITT. The results are represented as the mean ± SD (n = 10).

tolerance ($P < 0.001$). Simvastatin or CTS-200 mg/kg/day improved insulin tolerance ($P = 0.004$ and $P = 0.006$, respectively) (Fig. 2c, d). Furthermore, CTS-200 mg/kg/day significantly reduced the elevated fasting blood insulin level in HFD-fed mice ($P < 0.001$), while fasting blood glucose was not affected by CTS-200 mg/kg/d ($P = 0.412$) (Table 4). Hepatic FFA content and Ca^{2+}-Mg^{2+}-ATPase activity were significantly increased in the HFD-fed mice compared with those in normal controls ($P < 0.001$ and $P = 0.048$, respectively). Further, the FFA

Feng *et al. Chin Med* (2015) 10:23

Page 8 of 13

content and ATPase activity in the liver were highly significantly lower in mice treated with CTS-200 mg/kg/day compared with HFD-fed mice ($P < 0.001$ and $P = 0.001$, respectively) (Table 5).

CTS protect mouse liver against oxidative stress-mediated injury induced by lipid overload

The hepatic TBARS content was determined to evaluate lipid peroxidation levels in the liver and the anti-oxidative status (Table 5). Both results showed that CTS attenuated oxidative stress in the liver. The level of MDA in the liver was four times higher in the HFD group than in the untreated group ($P < 0.001$), and CTS-100 mg/kg/d markedly reduced the level of MDA (from 3.19 ± 0.33 to 1.68 ± 0.54). The level of GSH in the liver was lower in the HFD group than in the control group ($P < 0.001$). After 8 weeks of treatment, CTS (100 and 200 mg/kg/day) significantly increased the GSH level in the liver to a level comparable to that in the control group ($P < 0.001$ and $P < 0.001$, respectively). Plasma ALT and AST activities in different groups were examined to determine whether treatment with CTS could improve the HFD-induced liver injury. The activity of plasma ALT in the HFD group was significantly higher than that in the control group, and both simvastatin and CTS-200 mg/kg/d decreased ALT activity ($P < 0.001$ and $P < 0.001$, respectively). However, there was no significant difference in the level of plasma AST among these groups, except for that in the simvastatin group (Table 6). Hepatic lipids were measured by Oil O red staining and TG content analysis. HFD induced the formation of lipid droplets, which was ameliorated by simvastatin and CTS treatments (Fig. 3). These results suggested that CTS

treatment dose-dependently protected against liver damage by suppressing hepatic fat accumulation.

CTS activate AMPK phosphorylation and inhibit mRNA expression of SREBPs and their target genes

HFD-fed mice showed inhibition of AMPKα (Thr172) and ACC protein phosphorylation in the liver ($P < 0.001$ and $P = 0.001$, respectively), but AMPKα and ACC phosphorylation was restored after treatment with CTS-200 mg/kg/day for 8 weeks ($P = 0.011$ and $P < 0.001$, respectively). On the other hand, the mRNA levels of SREBP-1c, FAS, SCD-1, and ACC were significantly inhibited in the CTS-treated group ($P = 0.013$, $P = 0.011$, $P = 0.014$, and $P = 0.023$, respectively). Meanwhile, the expression of the genes in the cholesterol synthetic pathway, such as SREBP-2 and HMGCS, was significantly attenuated in the liver in comparison to that in the HFD-fed group ($P = 0.007$ and $P = 0.010$, respectively) (Fig. 4). Activation of the AMPK-mediated SREBP signaling pathway by CTS might be a potential mechanism underlying the suppression of hepatic fat accumulation.

Discussion

We showed that orally administered CTS (100 and 200 mg/kg/day) from *I. latifolia* could alleviate NAFLD in HFD-fed mice, and elucidated its underlying mechanisms of suppression of fat accumulation via AMPK pathway activation, to reduce body weight gain, hyperlipidemia, and IR in HFD-fed mice. The depletion of glutathione levels and lipid peroxidation in HFD-fed mice were inhibited by administration of CTS. ALT activity and histologic evidence in the liver showed that CTS treatment prevented liver injury caused by lipid accumulation. CTS

Table 5 Effects of CTS on FFA, MDA, GSH and ATPase in the livers of mice fed with HFD

Parameter	Control	HFD	HFD + Simvastatin	HFD + CTS-100	HFD + CTS-200
FFA (μmol/g protein)	61.05 ± 12.49	94.70 ± 15.63##	91.73 ± 13.50△	93.89 ± 10.81*	79.87 ± 11.18**
MDA (nmol/mg protein)	0.69 ± 0.34	3.19 ± 0.33##	1.88 ± 0.44△△	1.68 ± 0.54**	1.50 ± 0.38**
GSH (μg/mg protein)	2.65 ± 0.53	1.05 ± 0.24##	2.80 ± 0.59△△	2.55 ± 0.65**	2.61 ± 0.50**
Na+-K+-ATPase (mmol pi/g/h)	1.55 ± 0.19	1.79 ± 018#	1.57 ± 0.26△	1.68 ± 0.10	1.60 ± 0.26*
Ca2+-Mg2+-ATPase (mmol pi/g/h)	1.65 ± 0.13	1.76 ± 0.11#	1.31 ± 0.14△	1.55 ± 0.14**	1.42 ± 0.31**

Values were expressed as the mean ± SD (n = 10). # $P < 0.05$, ##$P < 0.01$, HFD vs. control. △$P < 0.05$, △△$P < 0.01$, HFD vs. simvastatin treatment. *$P < 0.05$, **$P < 0.01$, HFD vs. CTS treatment.

Table 6 Effects of CTS on plasma ALT and AST activities in mice fed with HFD

Parameter	Control	HFD	HFD + Simvastatin	HFD + CTS-100	HFD + CTS-200
ALT (KAIU/L)	43.15 ± 3.98	62.61 ± 14.81##	51.34 ± 15.81△△	50.94 ± 15.95**	40.74 ± 7.90**
AST (KAIU/L)	104.85 ± 26.20	101.74 ± 22.86	127.65 ± 11.83△△	96.24 ± 10.18	98.87 ± 12.61

Values were expressed as the mean ± SD (n = 10). # $P < 0.05$, ##$P < 0.01$, HFD vs. control. △$P < 0.05$,△△$P < 0.01$, HFD vs. simvastatin treatment. *$P < 0.05$, **$P < 0.01$, HFD vs. CTS treatment.

Feng *et al. Chin Med* (2015) 10:23

Page 9 of 13

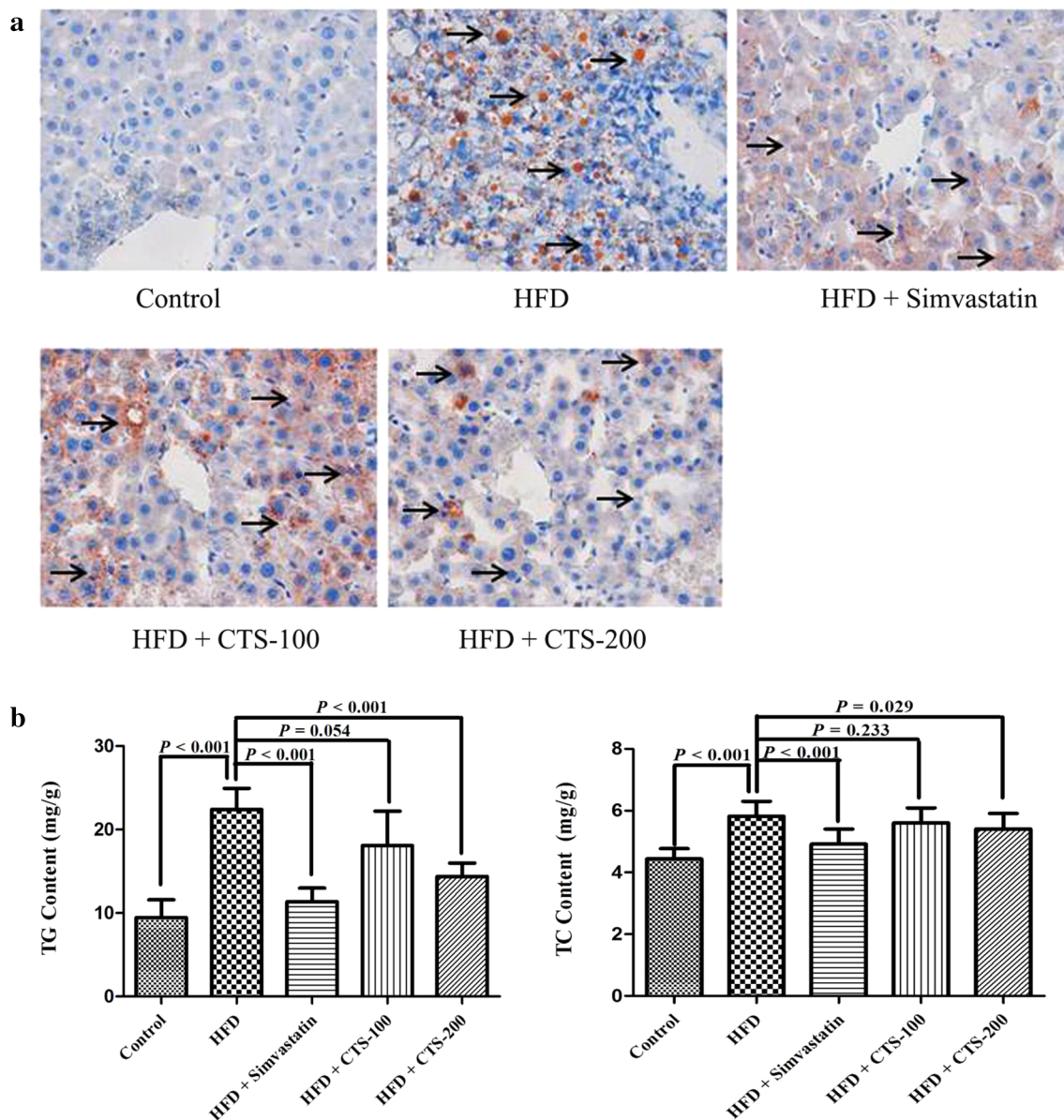**Fig. 3** Effects of CTS on liver injury and hepatic lipid content in HFD-fed mice. **a** Oil red O staining (×400) of the liver sections. Arrows indicate steatosis induced by HFD feeding. **b** The quantitative analysis of triglyceride (TG) and total cholesterol (TC) contents in livers. The HFD-fed mice were administered two concentrations of CTS (100 and 200 mg/kg/days) or the positive control simvastatin 10 mg/kg/d for 8 weeks. The results are represented as the mean ± SD (n = 10).

could activate AMPK and suppress expression of SREBPs and their target genes.

In previous studies *I. latifolia* was shown to exhibit anti-inflammatory and antioxidant effects and improve lipid metabolism [30, 31]. The water extract of *I. latifolia* inhibited hyperglycemia in rats with epinephrine-induced hyperglycemia [32], and increased the contractility and decreased the frequency of contraction in an isolated rat heart perfusion system by inhibiting Na^+/K^+-ATPase

activities [33]. Triterpenoid saponins such as ilekudinoside N and ilekudinoside Q from the aqueous extract of *I. kudingcha* reduced intracellular TC and TG contents in macrophages [34]. In addition, the CTS from the aqueous extract could significantly improve metabolic disorders in NAFLD mice [35].

In this study, an HFD-induced NAFLD mouse model was established according to previous research [29]. The HFD-fed group had higher body weight, fat accumulation
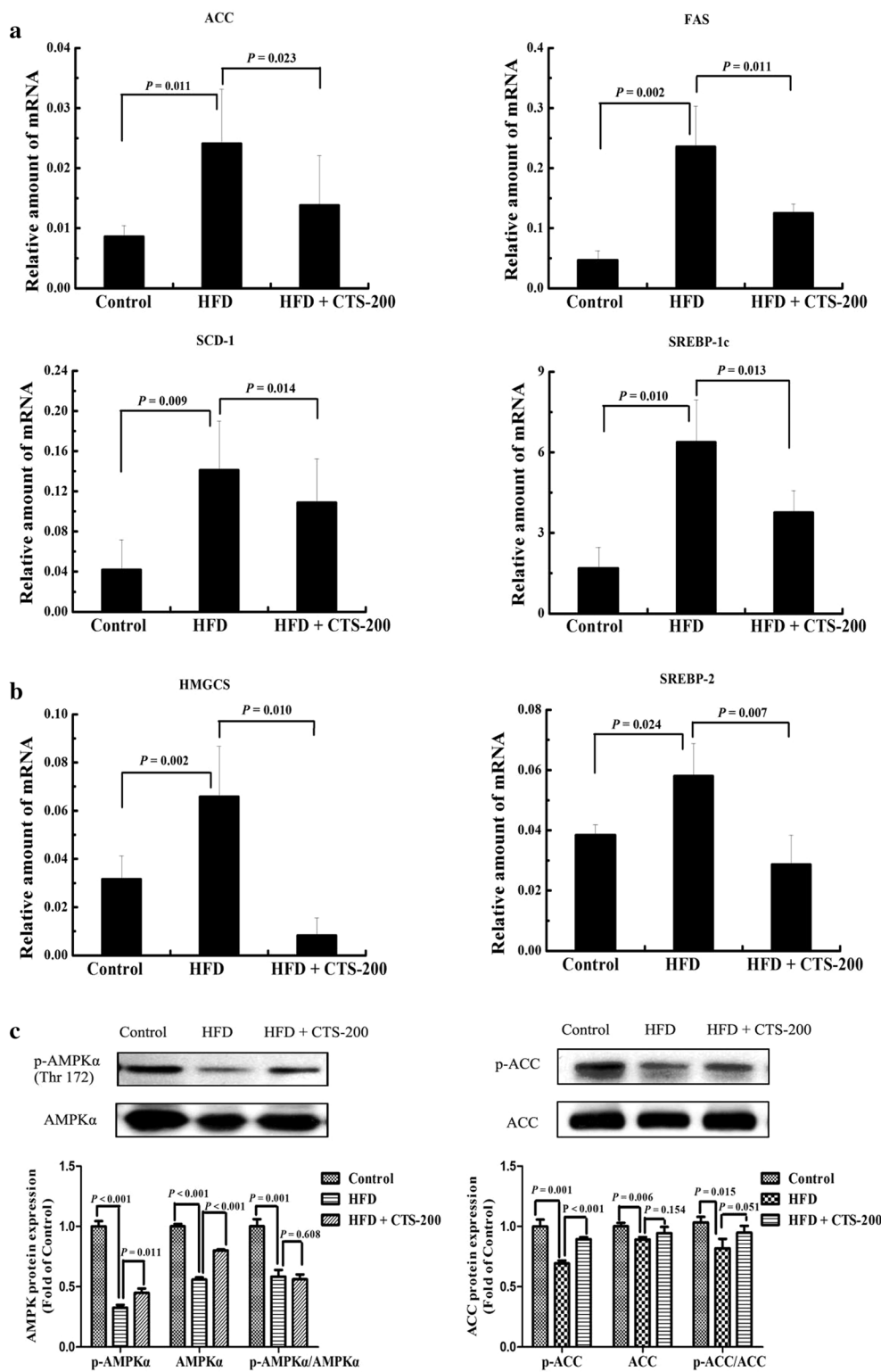
Feng *et al. Chin Med* (2015) 10:23

Page 10 of 13

Fig. 4 Effects of CTS on gene and protein expression of lipogenic and cholesterol-related synthetic enzymes. **a** The gene expression of lipogenic enzymes (SREBP-1c SCD1, ACC, FAS) in the livers of mice was suppressed by CTS-200 mg/kg/days. **b** The gene expression of cholesterol related synthetic enzymes (SREBP-2, HMGCS) in the livers of mice was suppressed by CTS-200 mg/kg/day. **c** Immunoblot analysis of phospho-AMPKα (Thr172), AMPK, phospho-ACC, and ACC protein. The protein levels are expressed as fold of control. All data were expressed as the mean ± SD (n = 10) of three independent experiments.

Feng *et al. Chin Med* (2015) 10:23

Page 11 of 13

in liver, and plasma levels of glucose and insulin compared with those in mice fed normal diets. Additionally, HFD caused a lipid metabolism disorder and disrupted the homeostasis of the liver oxidative state, which is an important characteristic in the development of NAFLD. Oral administration of CTS strongly prevented the development of NAFLD by significantly decreasing body and adipose tissue weights. Lipid accumulation in the liver frequently promoted the release of MDA, which diffused into other sites and favored oxidative stress [36, 37]. The increase in MDA content and decrease in GSH level could contribute to apoptosis and nuclear-mitochondrial DNA damage in NASH by producing reactive oxygen species (ROS) [37]. Our results demonstrated that CTS administration could reduce MDA content and restore GSH levels in the livers of HFD-fed mice. Plasma ALT levels indicated a protective effect of CTS on the liver.

IR is involved in the pathological process of NAFLD [38, 39]. Adipose tissue is insensitive to the anti-lipolytic effects of insulin in IR conditions, and the influx of exogenous FFA to the liver is increased. Circulating FFAs promote the production of intracellular metabolites (diacylglycerol), and produce dysfunctional cellular glucose [40]. In contrast, other studies have reported that IR and hyperinsulinemia are linked to the impairment of adenosine triphosphate (ATP) homeostasis [41, 42]. In the present study, the levels of insulin in HFD-fed mice were reduced significantly by CTS administration. Furthermore, CTS could improve HFD-induced glucose and IR. Moreover, CTS significantly reduced the levels of hepatic FFA and the activities of Na^+-K^+-ATPase and Ca^{2+}-Mg^{2+}-ATPase. These results suggested that CTS prevented pathological development of NAFLD by improving IR.

AMPK, an important energy sensor for cellular energy homeostasis, is recognized as a potential therapeutic target for the prevention and treatment of metabolic syndrome [43, 44]. The activation of AMPK in the liver could not only inhibit lipogenesis and gluconeogenesis but also stimulate fatty acid oxidation [45]. Natural products and drugs, such as resveratrol and metformin, could inhibit lipogenesis and eliminate hepatic steatosis in HFD-induced fatty liver by activating AMPK [46, 47]. Activated AMPK could bind phosphorylated SREBP-1c and SREBP-2, negatively regulating their proteolytic processing and elevating the expression levels of their target genes (*ACC*, *FAS*, *SCD1*, and *HMGCS*) in the livers of IR mice [42, 48]. The phosphorylation of AMPKα was activated by CTS treatment and the mRNA expression levels of SREBP-1c, FAS, SCD1, and ACC were reduced in the CTS-treated group. Meanwhile, CTS also suppressed the mRNA expression of SREBP2 and HMGCR, which are responsible for cholesterol biosynthesis [49]. CTS inhibited lipogenic synthesis and improved IR in HFD-fed mice by upregulating AMPK activation and suppressing the transcription of SREBPs and their target genes.

Conclusion

CTS from *I. latifolia* improved IR and liver injury in HFD-fed mice, and attenuated NAFLD via the activation of AMPK and inhibition of the gene expression of SREBPs and some of their target molecules.

Abbreviations

CTS: crude triterpenoid saponins; HFD: high-fat diet; NAFLD: non-alcoholic fatty liver disease; AMPK: AMP-activated protein kinase; NASH: non-alcoholic steatohepatitis; T2DM: type 2 diabetes mellitus; UHPLC-Q-TOF–MS: ultra-high performance liquid chromatography quadrupole time-of-flight tandem mass spectrometry; MCAO: middle cerebral artery occlusion; TBARS: thiobarbituric acid-reactive substances; RT-PCR: real-time reverse transcription polymerase chain reaction; AUC: area under the curve; SDS-PAGE: SDS-polyacrylamide gel electrophoresis; TG: triglycerides; ACC-1: CoA carboxylase-1; FAS: fatty acid synthase; SCD-1: stearoyl-CoA desaturase; SREBP-1c: sterol regulatory element-binding protein-1c; SREBP-2: sterol regulatory element-binding protein 2; HMGCS: hydroxymethylglutaryl coenzyme A synthase; OGTT: oral glucose tolerance test; ITT: insulin tolerance test; TC: Total cholesterol; LDL-c: low-density lipoprotein cholesterol; HDL-c: high-density lipoprotein cholesterol; ALT: aspartate aminotransferase; AST: alanine aminotransferase; FFA: free fatty acid; GSH: glutathione; MDA: malondialdehyde; ATPase: adenosine triphosphatase; ROS: reactive oxygen species; IR: insulin resistance.

Authors' contributions

WCY, MML and YW conceived and designed the study. RBF, CLF, MML, QL and ZL performed the experiments and collected the data. RBF, CLF, MML wrote the manuscript. WZ, YLL and WT revised the work. All authors read and approved the final manuscript.

Author details

[1] College of Pharmacy, Jinan University, Guangzhou 510632, People's Republic of China. [2] Guangdong Province Key Laboratory of Pharmacodynamic Constituents of TCM and New Drugs Research, Jinan University, Guangzhou 510632, People's Republic of China. [3] Guangzhou Jinan Biomedicine Research and Development Center, National Engineering Research Center of Genetic Medicine, Jinan University, Guangzhou 510632, People's Republic of China.

References
1. Petta S, Amato M, Di Marco V, Cammà C, Pizzolanti G, Barcellona M et al (2012) Visceral adiposity index is associated with significant fibrosis in patients with non-alcoholic fatty liver disease. Aliment Pharm Therap 35:238–247

Feng *et al. Chin Med* (2015) 10:23

Page 12 of 13

2. Wong RJ, Ahmed A (2014) Obesity and non-alcoholic fatty liver disease: disparate associations among Asian populations. World J Hepatol 6:263–273

3. Cauchy F, Fuks D, Zarzavadjian Le Bian A, Belghiti J, Costi R (2014) Metabolic syndrome and non-alcoholic fatty liver disease in liver surgery: the new scourges? World J Hepatol 6:306–314

4. Wu CL, Zhao SP, Yu BL (2015) Intracellular role of exchangeable apolipoproteins in energy homeostasis, obesity and non-alcoholic fatty liver disease. Biol Rev 90:367–376

5. Marzuillo P, Del Giudice EM, Santoro N (2014) Pediatric non-alcoholic fatty liver disease: new insights and future directions. World J Hepatol 6:217–225

6. Ozturk ZA, Kadayifci A (2014) Insulin sensitizers for the treatment of non-alcoholic fatty liver disease. World J Hepatol 6:199–206

7. Daemen S, Kutmon M, Evelo CT (2013) A pathway approach to investigate the function and regulation of SREBPs. Genes Nutr 8:289–300

8. Xiaoli YF (2013) Mediating lipid biosynthesis: implications for cardiovascular disease. Trends Cardiovasc Med 23:269–273

9. Faust PL, Kovacs WJ (2014) Cholesterol biosynthesis and ER stress in peroxisome deficiency. Biochimie 98:75–85

10. Kim YW, Kim YM, Yang YM, Kim TH, Hwang SJ, Lee JR et al (2010) Inhibition of SREBP-1c-mediated hepatic steatosis and oxidative stress by sauchinone, an AMPK-activating lignan in Saururus chinensis. Free Radical Bio Med 48:567–578

11. Lee HI, Yun KW, Seo KI, Kim MJ, Lee MK (2014) Scopoletin prevents alcohol-induced hepatic lipid accumulation by modulating the AMPK-SREBP pathway in diet-induced obese mice. Metabolism 63:593–601

12. Lu J, Huang G, Hu S, Wang Z, Guan S (2014) 1,3-Dichloro-2-propanol induced hyperlipidemia in C57BL/6J mice via AMPK signaling pathway. Food Chem Toxicol 64:403–409

13. Li Y, Xu S, Mihaylova MM, Zheng B, Hou X, Jiang B et al (2011) AMPK phosphorylates and inhibits SREBP activity to attenuate hepatic steatosis and atherosclerosis in diet-induced insulin-resistant mice. Cell Metab 13:376–388

14. Li L, Xu LJ, Ma GZ, Dong YM, Peng Y, Xiao PG (2013) The large-leaved Kudingcha (*Ilex latifolia* Thunb and Ilex kudingcha C.J. Tseng): a traditional Chinese tea with plentiful secondary metabolites and potential biological activities. J Nat Med 67:425–437

15. Huang J, Wang X, Ogihara Y, Shimizu N, Takeda T, Akiyama T (2001) Latifolosides I and J, two new triterpenoid saponins from the bark of *Ilex latifolia*. Chem Pharm Bull (Tokyo) 49:239–241

16. Chen Y, Li K, Xie T (1994) Hypotensive action of the extract of Kudingcha dongqingye (Ilex kudingcha). Chin Tradit Herb Drugs 26:250–252

17. Wang CQ, Wang L, Fan CL, Zhang DM, Huang XJ, Jiang RW et al (2012) Ilelic acids A and B, two unusual triterpenes with a seven-membered ring from *Ilex latifolia*. Org Lett 14:4102–4105

18. Zuo WJ, Dai HF, Chen J, Chen HQ, Zhao YX, Mei WL et al (2011) Triterpenes and triterpenoid saponins from the leaves of Ilex kudingcha. Planta Med 77:1835–1840

19. She GM, Wang D, Zeng SF, Yang CR, Zhang YJ (2008) New phenylethanoid glycosides and sugar esters from Ku-Ding-Cha, a herbal tea Produced from Ligustrum purpurascens. J Food Sci 73:476–481

20. Hao D, Gu X, Xiao P, Liang Z, Xu L, Peng Y (2013) Research progress in the phytochemistry and biology of Ilex pharmaceutical resources. Acta Pharmaceutica Sinica B 3:8–19

21. Kim JY, Jeong HY, Lee HK, Yoo JK, Bae K, Seong YH (2011) Protective effect of Ilex latifolia, a major component of "kudingcha", against transient focal ischemia-induced neuronal damage in rats. J Ethnopharmacol 133:558–564

22. Cignarella A, Fan S, Zhang Y, Hu N, Sun Q, Ding X et al (2012) Extract of kuding tea prevents high-fat diet-induced metabolic disorders in C57BL/6 mice via liver X receptor (LXR) β antagonism. PLoS One 7:1–12

23. Fan J, Wu Z, Zhao T, Sun Y, Ye H, Xu R et al (2014) Characterization, antioxidant and hepatoprotective activities of polysaccharides from *Ilex latifolia* Thunb. Carbohyd Polym 101:990–997

24. Nishimura K, Fukuda T, Miyase T, Noguchi H, Chen XM (1999) Activity-guided isolation of triterpenoid acyl CoA cholesteryl acyl transferase (ACAT) inhibitors from Ilex kudingcha. J Nat Prod 62:1061–1064

25. Nishimura K, Miyase T, Noguchi H (1999) Triterpenoid saponins from Ilex kudingcha. J Nat Prod 62:1128–1133

26. Fan C, Fan L, Zhang X, Wang Y, Zhang J, Ye W (2010) Triterpenoid saponins from the leaves of *Ilex latifolia*. Chin Pharm J. 45:1228–1232

27. Ouyang M, Wang H, Liu Y, Yang C (1997) Triterpenoid saponins from the leaves of *Ilex latifolia*. Phytochemistry 45:1501–1505

28. Fan C, Deng J, Yang Y, Liu J, Wang Y, Zhang X et al (2013) Multi-ingredients determination and fingerprint analysis of leaves from *Ilex latifolia* using ultra-performance liquid chromatography coupled with quadrupole time-of-flight mass spectrometry. J Pharm Biomed Anal 84:20–29

29. Tang J, Li J, Qi W, Qiu W, Li P, Li B et al (2011) Inhibition of SREBP by a small molecule, betulin, improves hyperlipidemia and insulin resistance and reduces atherosclerotic plaques. Cell Metab 13:44–56

30. Li L, Peng Y, Ma G, He C, Feng Y, Lei Q et al (2012) Quantitative analysis of five kudinosides in the large-leaved Kudingcha and related species from the genus Ilex by UPLC-ELSD. Phytochem Anal 23:677–683

31. Hu T, He XW, Jiang JG, Xu XL (2014) Efficacy evaluation of a Chinese bitter tea (*Ilex latifolia* Thunb.) via analyses of its main components. Food Funct 5:876–881

32. Qu LZ, Lu T, Lu PJ, Xi J (1999) The effect of Kudingcha on epinephrine hyperglycemia rats. Tradit Chin Drug Res Clin Pharmacol 10:279–280

33. Woo AY, Jiang JM, Chau CF, Waye MM, Cheung WT, Kwan HS et al (2001) Inotropic and chronotropic actions of Ilex latifolia inhibition of adenosine-5′-triphosphatases as a possible mechanism. Life Sci 68:1259–1270

34. Zheng J, Tang L, Xian XD, Zhou SX, Shi HM, Jiang Y et al (2009) Inhibitory effect of triterpenoid saponins from the leaves of Ilex kudingcha on aggregated LDL-induced lipid deposition in macrophages. Planta Med 75:1410–1414

35. Pan H, Liao Z, Ying Q, Tian J, Xu Y (2004) Study on lipid-depressing function of kuding tea prepared from *Ilex latifolia* Thunb leaves. J Tea Sci 24:49–52

36. Ferro E, Visalli G, Civa R, La Rosa MA, Randazzo Papa G, Baluce B et al (2012) Oxidative damage and genotoxicity biomarkers in transfused and untransfused thalassemic subjects. Free Radic Biol Med 53:1829–1837

37. Takaki A, Kawai D, Yamamoto K (2013) Multiple hits, including oxidative stress, as pathogenesis and treatment target in non-alcoholic steatohepatitis (NASH). Int J Mol Sci 14:20704–20728

38. Milic S, Lulic D, Stimac D (2014) Non-alcoholic fatty liver disease and obesity: biochemical, metabolic and clinical presentations. World J Gastroenterol 20:9330–9337

39. Pala L, Barbaro V, Dicembrini I, Rotella CM (2014) The therapy of insulin resistance in other diseases besides type 2 diabetes. Eat Weight Disord. 19:275–283

40. Tarantino G, Saldalamacchia G, Conca P, Arena A (2007) Non-alcoholic fatty liver disease: further expression of the metabolic syndrome. J Gastroenterol Hepatol 22:293–303

41. Hui E, Xu A, Bo Yang H, Lam KS (2013) Obesity as the common soil of non-alcoholic fatty liver disease and diabetes: role of adipokines. J Diabetes Investig 4:413–425

42. Pasarin M, Abraldes JG, Rodriguez-Vilarrupla A, La Mura V, Garcia-Pagan JC, Bosch J (2011) Insulin resistance and liver microcirculation in a rat model of early NAFLD. J Hepatol 55:1095–1102

43. Kahn BB, Alquier T, Carling D, Hardie DG (2005) AMP-activated protein kinase: ancient energy gauge provides clues to modern understanding of metabolism. Cell Metab 1:15–25

44. Grahame Hardie D (2014) AMP-activated protein kinase: a key regulator of energy balance with many roles in human disease. J Intern Med 276:543–559

45. Viollet B, Foretz M, Guigas B, Horman S, Dentin R, Bertrand L et al (2006) Activation of AMP-activated protein kinase in the liver: a new strategy for the management of metabolic hepatic disorders. J Physiol 574:41–53

46. Jeon BT, Jeong EA, Shin HJ, Lee Y, Lee DH, Kim HJ et al (2012) Resveratrol attenuates obesity-associated peripheral and central inflammation and improves memory deficit in mice fed a high-fat diet. Diabetes 61:1444–1454

47. Caton P, Kieswich J, Yaqoob M, Holness M, Sugden M (2011) Metformin opposes impaired AMPK and SIRT1 function and deleterious changes in core clock protein expression in white adipose tissue of genetically-obese db/db mice. Diabetes Obes Metab 13:1097–1104

Feng *et al. Chin Med* (2015) 10:23

Page 13 of 13

48. Soetikno V, Sari FR, Sukumaran V, Lakshmanan AP, Harima M, Suzuki K et al (2013) Curcumin decreases renal triglyceride accumulation through AMPK-SREBP signaling pathway in streptozotocin-induced type 1 diabetic rats. J Nutr Biochem 24:796–802

49. Min H-K, Kapoor A, Fuchs M, Mirshahi F, Zhou H, Maher J et al (2012) Increased hepatic synthesis and dysregulation of cholesterol metabolism is associated with the severity of nonalcoholic fatty liver disease. Cell Metab 15:665–674